33rd Annual International Conference of the IEEE EMBS
Boston, Massachusetts USA, August 30 - September 3, 2011

Computerized Detection of Peripapillary Chorioretinal Atrophy by Texture Analysis

Chisako Muramatsu, Yuji Hatanaka, Akira Sawada, Tetsuya Yamamoto,
and Hiroshi Fujita, *Member, IEEE*

***Abstract*—Presence of peripapillary chorioretinal atrophy (PPA) is considered one of the risk factors for glaucoma. It can be identified as bright regions in retinal fundus images, and therefore, incorrectly included as the part of the optic disc regions in the automated disc detection scheme. For potential risk assessment and use in improving optic disc segmentation, a computerized detection of PPA was investigated. By using texture analysis, the sensitivity for detecting the moderate to severe PPA regions in the test dataset was 73% with the specificity of 95%. The proposed method may be useful for identifying the cases with the PPA in retinal fundus images.**

I. Introduction

GLAUCOMA is the second leading cause of vision loss in the world [1]. Early detection is a key factor for avoiding permanent blindness. In a population-based prevalence survery of glaucoma in Tajimi, Japan, 93% of those who were diagnosed with glaucoma were newly diagnosed [2]. Because of its slow progressive nature, many patients stay unaware of the disease. Retinal examination using fundus photographs can be used for screening glaucoma.

In the screening examination, physicians must read a large number of images in a limited time. To help increasing the efficiency in their diagnosis, we have been investigating computerized schemes to detect diagnostic signs or to quantify diagnostic indices, such as a cup-to-disc ratio (CDR), on retinal fundus images [3]-[5]. In the computer analysis of retinal fundus images, it is often desired that optical nerve head is detected. When measuring the CDR, the optic nerve head must be outlined for determining its diameter. In our previous study, we investigated automated methods for segmenting the optic discs [6]. In most cases, the segmentation was reasonably successful in comparison with the manual outlines by an ophthalmologist. However, in some cases, the methods over-segmented areas of peripapillary chorioretinal atrophy (PPA), because of its bright characteristic.

For improving the segmentation accuracy and CDR measurement, identification of the PPA regions is desirable. In addition, since the PPA is considered one of the risk factors for glaucoma [7], automated detection of PPA may be helpful for the glaucoma diagnosis. To our knowledge, there has been no study targeted to the automatic detection of PPA. As an initial investigation, our objective is to detect moderate to severe PPA β-type, which can be related to glaucoma and also mistakenly included in the disc segmentation. On the basis of its appearance, as shown in Fig. 1, automated detection of PPA by using texture analysis was investigated in this study.

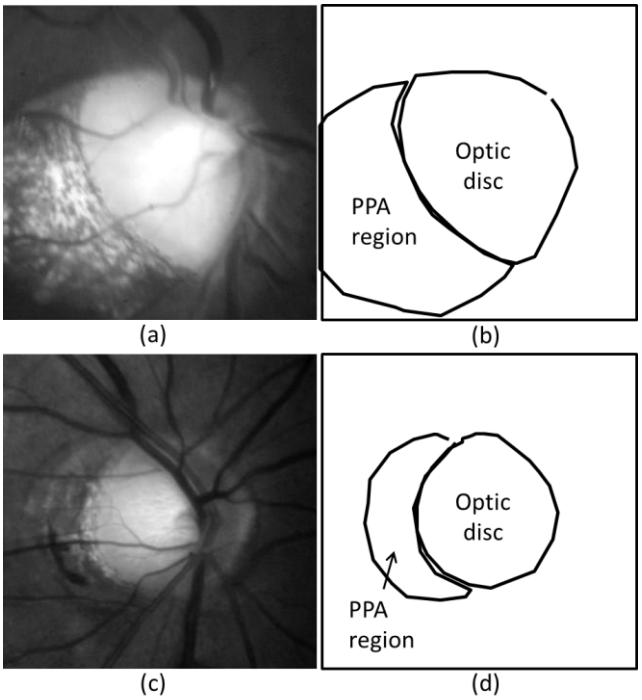

Fig. 1. ROIs with peripapillary chorioretinal atrophy (PPA) regions: (a) an image with severe PPA, (c) an image with mild PPA, and (b), (d) their approximate areas

II. Dataset

A. Training Dataset

The training dataset included 80 retinal fundus images which were obtained using a stereo retinal fundus camera (a prototype of the WX-1, Kowa Company, Ltd., Tokyo, Japan).

Manuscript received March 26, 2011. This study is partly supported by the Computational Anatomy for Computer-aided Diagnosis and Therapy by Grant-in-Aid for Scientific Research on Innovative Areas, MEXT, Japan.

C. Muramatsu and H. Fujita are with the Department of Intelligent Image Information, Graduate School of Medicine, Gifu University, Gifu, 501-1194 Japan (phone: 81-58-230-6519; fax: 81-58-230-6514; e-mail: chisa@fjt.info.gifu-u.ac.jp; fujita@fjt.info.gifu-u.ac.jp).

Y. Hatanaka is with the Department of Electronic System Engineering, School of Engineeing, the University of Shiga Prefecture, Shiga, 522-8533 Japan (e-mail: hatanaka.y@usp.ac.jp).

A. Sawada and T. Yamamoto are with the Department of Ophthalmology, Graduate School of Medicine, Gifu University, Gifu, 501-1194 Japan (e-mail: sawada-gif@umin.ac.jp; mmc-gif@umin.net).

For observing the optic nerve head condition, these images were pictured with a 27° optic angle centered at optic nerve head. The images were saved in JPEG format with a 1600 x 1200 pixel resolution. Although a pair of images was taken from each individual, only the first photograph of the pair was used in this study. These images include 25 cases with signs of glaucoma and 55 cases without the signs according to ophthalmologist's findings. Eight cases were considered having moderate to severe PPA, in which sclera is exposed and choroidal vessels may be observed. Of these, six cases were in the glaucomatous eye group. This dataset was used for determining parameters for a classifier and false positive reduction rules.

B. Test Dataset

Another dataset of 91 retinal fundus images were obtained with the same camera system, which were used for evaluating the detection scheme. The dataset includes 58 cases with signs of glaucoma and 33 cases without the signs. Twenty six cases were considered having moderate to severe PPA. Two cases out of 26 cases were considered having no sign of glaucoma.

III. Procedure for PPA Detection

For detection of PPA, a texture analysis based on the gray level co-occurrence matrix (GLCM) [8], [9] was used. In this study, regions of interest (ROIs) containing the optic discs were only processed. The ROIs of 600 x 600 pixels in size were extracted automatically by identifying the approximate disc locations using a p-tile thresholding method [10] for precise segmentation of disc regions in our previous study [6]. Although parts of the PPA regions may be outside the ROIs in some cases, the regions outside the ROIs were disregarded in this initial investigation which purposes are to detect PPA for risk analysis and exclude the PPA regions in the disc segmentation. In future study, larger areas may be included.

First, the ROIs were down-sampled to 150 x 150 pixels by pixel averaging for reducing computational expense. The number of gray scales was reduced from 256 to 32 levels. At each pixel, the GLCM was calculated in the surrounding 25 x 25 pixel area for three color planes, i.e., red, green, and blue, with the following equation [9];

$$P(i,j,d,\theta) = \#\{(x_1,y_1)(x_2,y_2) \mid f(x_1,y_1)=i, \; f(x_2,y_2)=j, \mid (x_1,y_1)-(x_2,y_2)\mid = d, \; \angle((x_1,y_1),(x_2,y_2))=\theta\}. \quad (1)$$

They were determined for $d = 1$ and $\theta = 0°$, 45°, 90°, and 135°. Other combinations of scales for down-sampling, areas for determining the GLCM, and d were tested with a small number of training cases, and the above mentioned parameters were selected. On the basis of the GLCM, textural features were calculated, including angular second moment (ASM), contrast, correlation, variance, inverse difference moment (IDM), entropy, and dissimilarity. The definitions for these features were provided elsewhere [8], [9]. For each feature, the mean, maximum, and minimum values of four angles were determined.

TABLE I
SELECTED FEATURES AND THEIR F-VALUES FOR TESTING THE DIFFERENCES BETWEEN MEANS

Feature	Mean/ maximum/minimum	F-value
Contrast	Minimum	5080
Correlation	Maximum	2187
Variance	Maximum	260
Inverse difference moment	Maximum	4224
Entropy	Minimum	4413
Dissimilarity	Maximum	2673

With the textural features, classification of PPA pixels and non-PPA pixels was performed using a linear discriminant analysis (LDA). For determining LDA parameters with the IBM SPSS Statistics software version 19.0, the pixels from the eight images with PPA in the training set were used. The classifier was trained using different combinations of features, such as the features from each color plane, the features from three color planes, the mean, maximum or minimum features separately, and all together, with a stepwise feature selection.

When the mean, maximum, and minimum of 7 features from 3 color planes, thus a total of 63 features, were used as input data, 27 features were selected, and 88.8% of the pixels in the 8 cases were classified correctly. However, it was predicted that the test result would be suboptimal because of the large number of features. When the mean, maximum, or minimum features of the 3 color planes were input separately, 17, 19, and 19 features, respectively, were selected. The classification accuracies in the 8 training cases were 82.5%, 87.5%, and 87.9%, respectively. Because the features from the blue and green planes were correlated ($r > 0.75$), reduction of the number of features by selecting one color for each texture feature did not result in a large loss of accuracy (approximately 84%).

Instead, when the mean, maximum, and minimum features of the blue planes were used, 11 features were selected and the classification accuracies were 82.4%. Although using the features from the three color planes provided better classification accuracies, it led to a large number of false positives in non-PPA cases in the training set which were not used in the LDA training. Because the mean, maximum, and minimum of each feature are highly correlated ($r > 0.95$), when 11 features were reduced to 6 features by selecting the one with the highest F-value for each, the classification accuracy decreased only slightly to 79.4%. Therefore, 6 features from the blue plane were selected, as listed in Table 1, for the LDA. None of the second angular moment features were selected by the stepwise feature selection. The F-values for testing the differences between means are also listed. The distributions of the PPA and non-PPA pixels in the minimum

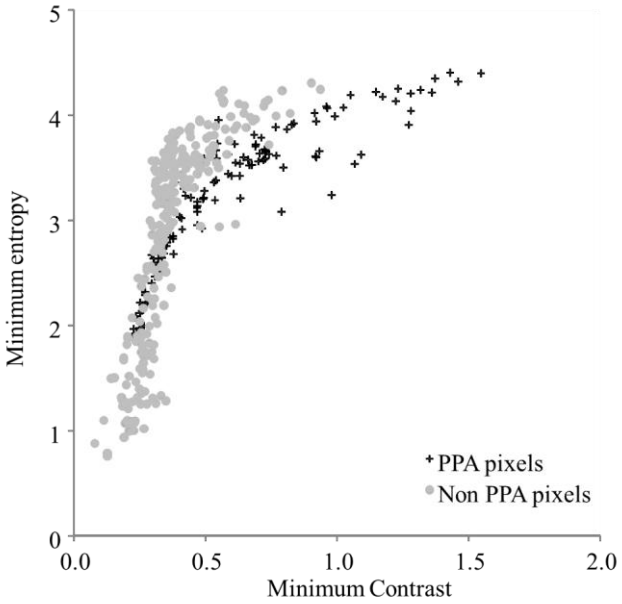

Fig. 2. Distributions of PPA pixels and non-PPA pixels in the texture features with the high F-values

contrast and the maximum entropy are shown in Fig. 2. They are sampled from the image in Fig. 1(a). Even with the features with such high F-values, the distributions are substantially overlapped, indicating the difficulty of classifying marginal pixels.

The ROIs were binarized on the basis of the outputs from the LDA with a threshold, which was determined empirically. The small regions with the area smaller than 300 pixels were considered as false positives and removed. The PPA regions must be adjacent to the optic disc regions. Therefore, for each candidate region, the fraction of the pixels that were in contact with the disc border was calculated. A candidate region was removed if the fraction is smaller than 3%, if the region is overlapped with more than a half of the disc region, or if the center of the region is very close to the center of disc region. For this rule, the disc segmentation result in the previous study was used [6]; in this method, the disc outline was determined by use of an active contour model [11] based on the edges detected by the Canny filter [12].

After applying these rules to the training set, PPAs in 7 out of 8 cases were detected (sensitivity of 88%) with 11 false positives in the non-PPA cases (specificity of 85%). In one missed case, a small region was detected which was only slightly overlapped with the gold standard region, and therefore, considered as non-detection. In this preliminary investigation, if more than a half of the detected region is overlapped with the PPA region, it was considered as the true detection. The detection scheme was applied to the test dataset.

IV. Results and Discussion

Out of 26 test images with moderate to severe PPA, 19 were detected correctly (sensitivity of 73%). Fig. 3 shows the images with PPA that were detected and missed. For two of the seven PPA regions that were not detected, only small parts of the PPA regions were detected as the result of the LDA, and therefore, removed by the small-region rule. In another three cases, the initial detection regions were removed because the large parts of the disc regions were also included with the PPA regions. The PPA pixels were not detected in one case as the result of LDA. In the remaining case, almost the entire ROI regions were classified as the PPA region, which may be due to the image normalization problem. For correctly detecting some of these cases, the LDA parameters must be adjusted, and the set of false positive reduction rules must to be refined.

Although considered as moderate to severe PPA cases, these cases often include some regions with mild characteristics. In this study, the gold standard PPA regions were slightly shrunk by the erosion operation for excluding the marginal regions, while they were enlarged by the dilation operation for sampling of the "normal" pixels. However, when determining texture features in the surround 25 x 25 pixel regions, some normal pixels may be included in the PPA regions, and some PPA regions may be included in the normal regions. Therefore, the LDA training could be suboptimal because of the mixed characteristics of PPA and non-PPA regions. In this study, our target was to detect moderate to severe PPA regions. However, in the future, it may be useful to detect mild PPA regions for the glaucoma risk analysis.

The false positive detections were present in 3 of 91 cases (specificity of 94%). In all of these 3 cases, parts of the optic disc regions were detected, including retinal blood vessels as shown in Fig. 3(d). Although the texture characteristics of the

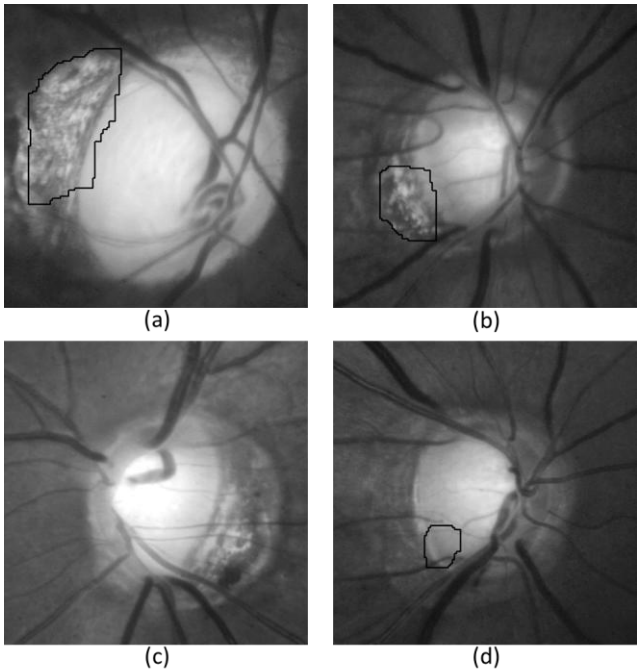

Fig. 3. PPA detection results: (a) true detection in the image with severe PPA, (b) detection in the image with moderate PPA, (c) false negative detection in the image with moderate PPA, and (d) false positive detection in the disc region

PPA regions and these regions seem very different, they were classified as the PPA pixels by the LDA. Further investigation is needed to more accurately determine the texture features for improving the classification accuracy.

In this study, the detected PPA regions often included parts of the optic disc regions, as shown in Fig. 3(a) and (b). For purpose of excluding PPA regions from optic disc segmentation, the PPA regions must be more accurately determined. In the future, a different approach or an additional method should be investigated for determining the exact border between two regions.

V. Conclusion

This was our initial study for automatic detection of PPA regions in retinal fundus images. The usefulness of the texture analysis in detecting the PPA regions was investigated. The result indicates that the texture analysis may be useful for identifying at least a part of the PPA regions. Further improvement is needed for improving sensitivity for mild to severe PPA and for precisely determining PPA regions to improve the optic disc segmentation.

References

[1] H. A. Quigley, "Number of people with glaucoma worldwide," *Br. J. Ophthalmo*.,. vol. 80, pp. 389-393, 1996.

[2] A. Iwase, Y. Suzuki, M. Araie, T. Yamamoto, H. Abe, S. Shirato, Y. Kuwayama, H. K. Mishima, H. Shimizu, G. Tomita, Y. Inoue, and Y. Kitazawa, "The prevalence of primary open-angle glaucoma in Japanese: the Tajimi Study," *Ophthalmology,* vol. 111, pp. 1641-1648, 2004.

[3] C. Muramatsu, Y. Hayashi, A. Sawada, Y. Hatanaka T. Hara, T. Yamamoto, and H. Fujita, "Detection of retinal nerve fiber layer defects on retinal fundus images for early diagnosis of glaucoma," *J. Biomed. Optics*, vol. 15, pp. 016021-1-7, Jan./Feb. 2010.

[4] C. Muramatsu, T. Nakagawa, A. Sawada, Y. Hatanaka, T. Hara, T. Yamamoto, and H. Fujita, "Determination of cup and disc ratio of optical nerve head for diagnosis of glaucoma on stereo retinal fundus image pairs," *Proc. SPIE Med. Imaging*, vol. 7260, pp. 72603L-1-8, 2009.

[5] Y. Hatanaka, A. Noudo, C. Muramatsu, A. Sawada, T. Hara, T. Yamamoto, and H. Fujita, "Vertical cup-to-disc ratio measurement for diagnosis of glaucoma on fundus images," *Proc. SPIE Med. Imaging*, vol. 7624, pp. 76243C-1-8, 2010.

[6] C. Muramatsu, T. Nakagawa, A. Sawada, Y. Hatanaka, T. Hara, T. Yamamoto, and H. Fujita, "Automated segmentation of optic disc region on retinal fundus photographs: comparison of contour modeling and pixel classification methods," *Comput. Meth. Prog. Bio.*, vol. 101, pp. 23-32, Jan. 2011.

[7] G. Tomais, G. Georgopoulos, C. Koutsandrea, and M. Moschos, "Correlation of central corneal thickness and axial length to the optic disc and peripapillary atrophy among healthy individuals, glaucoma and ocular hypertension patients," *Clin. Ophthalmol.*, vol. 2, pp. 981–988, 2008.

[8] R. M. Haralick, K. Shanmugam, and I. Dinstein, "Textural features for image classification," *IEEE Trans. on Systems, Man, and Cybernetics*, vol. SMC-3, pp. 610-621, 1973.

[9] M. A. Tahir, A. Bouridane, and F. Kurugollu, "An FPGA based coprocessor for GLCM and Haralick texture features and their application in prostate cancer classification," *Analog Intergrated Circuits and Signal Processing*, vol. 43, pp. 205-215, 2005.

[10] J. R. Parker, *Algorithms for Image Processing and Computer Vision.* New York, NY: Wiley Computer Publishing, 1997, pp. 116–127.

[11] M. Kass, A. Witkin, and D. Terzopoulos, "Snakes: active contour models," *Int. J. Comput. Vis.,* vol. 1, pp. 321–331, 1988.

[12] J. Serra, "Introduction to mathematical morphology," *Comput. Vis. Graph Image Process,* vol. 35, pp. 283–305, 1986.